# Necrostatin-1 prevents skeletal muscle ischemia reperfusion injury by regulating Bok-mediated apoptosis

**Yu Cao[a], Hong-Bo Wang[a], Chun-Jue Ni[a], Shun-Li Chen[a], Wan-Tie Wang[b], Liang-Rong Wang[a,*]**

*[a]Department of Anesthesiology, The First Affiliated Hospital of Wenzhou Medical University, Zhejiang, China; [b]Institute of Ischemia-Reperfusion Injury, Wenzhou Medical University, Zhejiang, China.*

## Abstract

**Background:** Receptor interacting serine/threonine kinase 1 (RIPK1) mediates apoptosis by regulating the classic proapoptotic effectors Bcl-2-associated X protein (Bax) and Bcl-2 homologous antagonist/killer (Bak). Although Bcl-2-related ovarian killer (Bok) is structurally similar to Bak and Bax, it is unclear whether it mediates apoptosis in skeletal muscle ischemia reperfusion (IR) injury. We hypothesized that by regulating Bok-mediated apoptosis, inhibiting RIPK1 with necrostatin-1 would reduce skeletal muscle IR injury.

**Methods:** Rats were randomized into four groups: sham (SM), IR, IR treated with necrostatin-1 (NI), or vehicle dimethyl sulfoxide (DI). For the IR group, the right femoral artery was clamped for 4 hours and then reperfused for 4 hours, and for the NI and DI groups, necrostatin-1 (1.65 mg/kg) and the equal volume of dimethyl sulfoxide were intraperitoneally administered prior to IR induction. The structural damage of muscle tissue and protein expression of Bok, Bcl-2, and cleaved caspase-3 were investigated, and apoptotic cells were identified with terminal dUTP nick-end labeling (TUNEL) staining. In vitro, human skeletal muscle cells (HSMCs) were exposed to 6 hours of oxygen-glucose deprivation followed by normoxia for 6 hours to establish an oxygen-glucose deprivation/reoxygenation (OGD/R) model. To determine the role of Bok, cell viability, lactate dehydrogenase (LDH) release, and flow cytometry were examined to demonstrate the effects of necrostatin-1 and Bok knockdown on the OGD/R insult of HSMCs.

**Results:** Necrostatin-1 pretreatment markedly reduced IR-induced muscle damage and RIPK1, Bok, and cleaved caspase-3 expression, whereas upregualted Bcl-2 expression ($p < 0.05$). Furthermore, necrostatin-1 prevented mitochondrial damage and decreased TUNEL-positive muscle cells ($p < 0.05$). In vitro, HSMCs treated with necrostatin-1 showed reduced Bok expression, increased cell viability, and reduced LDH release in response to OGD/R ($p < 0.05$), and Bok knockdown significantly blunted the OGD/R insult in HSMCs.

**Conclusion:** Necrostatin-1 prevents skeletal muscle from IR injury by regulating Bok-mediated apoptosis.

**Keywords:** apoptosis; Bcl-2-related ovarian killer; Necrostatin-1; Receptor interacting protein 1; Reperfusion injury

## 1. INTRODUCTION

In terms of the sequence and structure, Bcl-2-related ovarian killer (Bok), a member of the B-cell lymphoma-2 (Bcl-2) family, is similar to the classic proapoptotic effectors Bcl-2-associated X protein (Bax) and Bcl-2 homologous antagonist/killer (Bak).[1,2] Overexpression of Bok results in permeablization of the mitochondrial outer membrane, activation of caspase-3, and ultimate death in a variety of cell systems.[1–3] Nonetheless, considering the deficiency of clarifying the upstream triggers and molecules, the role played by Bok in apoptosis is not well-defined.

Receptor interacting serine/threonine kinase 1 (RIPK1), a core regulator of necroptosis, matters considerably in regulating inflammatory response, and triggering multiple cell death pathways including apoptosis.[4,5] RIPK1 mediates nuclear factor kappa-B (NF-κB) activation that enhances the expression of various proinflammatory cytokines,[6] and necrostatin-1 (Nec-1), a specific inhibitor of RIPK1, is well-demonstrated to suppress inflammation.[7–9] Besides, RIPK1 is also involved in regulating apoptosis, and inhibiting RIPK1 with Nec-1 has been demonstrated to prevent apoptosis by inhibiting caspase-3 and Bax and enhancing Bcl-2 activity,[10] the effects of which on Bok-mediated apoptosis, however, remain unknown.

The present study aimed to investigate the effects of Nec-1 on rats with skeletal muscle ischemia reperfusion (IR), and Bok was depleted in human skeletal muscle cells (HSMCs) to clarify its potential role in mediating apoptosis following oxygen-glucose deprivation/reoxygenation (OGD/R)-induced RIPK1 activation. It was hypothesized that inhibiting RIPK1 with Nec-1 suppressed apoptosis by targeting the proapoptotic effector Bok in IR-induced skeletal muscle injury.

* *Address Correspondence. Dr. Liang-Rong Wang, Department of Anesthesiology, the First Affiliated Hospital of Wenzhou Medical University, Wenzhou 325000, Zhejiang Province, China. E-mail address: arerong1984@126.com (L.-R. Wang).*

*Conflicts of interest: The authors declare that they have no conflicts of interest related to the subject matter or materials discussed in this article.*

*Journal of Chinese Medical Association. (2023) 86: 26-33.*

*Received May 30, 2022; accepted July 8, 2022.*

*doi: 10.1097/JCMA.0000000000000806.*

## 2. METHODS

### 2.1. Animals

Our research protocols were in accordance with the National Institutes of Health's Guide for the Care and Use of Laboratory Animals and approved by The Animal Ethics Committee of the First Affiliated Hospital of Wenzhou Medical University. Twenty-four adult Sprague-Dawley rats weighing 180–220 g were purchased from Laboratory Animal Center at Wenzhou Medical University and were caged in a temperature- and humidity-controlled facility with a 12:12 h light/dark cycle and free access to standard animal feed and water.

Using a computer-generated table of random numbers (www.random.org), the rats were randomly assigned to one of four groups (n = 6), that is, sham (SM) group, IR group, ischemia reperfusion treated with Nec-1 (NI), or vehicle dimethyl sulfoxide (DI) group. To summarize, the IR group received 4 hours of ischemia and another 4 hours of reperfusion in the right hindlimb, whereas the SM group experienced a sham surgical procedure without femoral artery being clamped. The rats in the NI group received intraperitoneal administration of Nec-1 (1.65 mg/kg in 2% dimethyl sulfoxide; Selleck, Houston, TX) 60 minutes prior to the initiation of IR, while those in the DI group received an equal volume of the vehicle dimethyl sulfoxide instead in the same manner.

### 2.2. Rat model of skeletal muscle IR

Intraperitoneal injections of ketamine hydrochloride (80 mg/kg) and xylazine hydrochloride (13.5 mg/kg) were used for anesthetizing the rats. Following an incision in the right groin, skeletal muscle ischemia was induced by clamping the right femoral artery for 4 hours with an atraumatic clamp and meanwhile a rubber was placed to the right greater trochanter to prevent collateral circulation. The rats were anesthetized under a heat lamp throughout the ischemia period, and the incision was temporarily covered with a plastic sheet to prevent excessive dehydration. After 4 hours of ischemia, the clamp and rubber were removed, and the right hindlimb was allowed to perfuse for 4 hours. The incision was closed with sutures and received local infiltration with ropivacaine for analgesia. Besides, the rats were permitted to remain awake during the reperfusion phase. The ischemia and reperfusion were visually confirmed by changes in the color of the hind paws. At the end of the procedure, the animals were euthanized by the anesthetic overdose, and midline abdominal incision was immediately performed to collect abdominal aortic blood samples, while the ipsilateral gastrocnemius muscle samples were obtained for further detections.

### 2.3. Cell culture and treatment

HSMCs were purchased from iCell Bioscience Inc. (CAT NO. Hum-iCell-1236P; Shanghai, China) and cultured in Dulbecco's modified Eagle's medium (DMEM; Invitrogen, Inc., Carlsbad, CA, USA) supplemented with 10% fetal bovine serum (Invitrogen, Inc., Carlsbad, CA, USA) in 5% $CO_2$ at 37°C.

The cells were randomly divided into five groups: (1) control group (CN group): cells cultured under normoxic conditions; (2) OGD/R-treated group (HR group): cells exposed to 12 hours of oxygen-glucose deprivation followed by 18 hours of reoxygenation; (3) Nec-1 + OGD/R group (NH group): cells cocultured with Nec-1 50 μM for 24 hours under normoxic conditions before OGD/R insult; (4) Bok siRNA+ OGD/R group (siBok group): cells cocultured with small interfering RNA (siRNA) targeting Bok for 24 hours under normoxic conditions before OGD/R insult; (5) negative control siRNA + OGD/R group (siNC group): cells cocultured with negative control siRNA for 24 hours under normoxic conditions before OGD/R insult.

### 2.4. siRNA transfection

siRNA targeting human Bok (*5′-AAAAGAATTCCGGATGGACTGATGTCCTCAAGTGTGTCAAGAGCACACTTGAGGACATCAGTCCATCCTTTTTGCGGCCGCAAAA-3′*) and the negative control were synthesized in RiboBio Co., Ltd. (Guangzhou, China).[11] According to the manufacturer's instructions, HSMCs were seeded in a 96-well plate and transfected with the siRNAs using Lipofectamine 2000 (Thermo Fisher Scientific, Waltham, MA, USA). Afterwards, the transfection efficacy was confirmed by Western blot assay.

### 2.5. OGD/R treatment

The OGD/R insult was performed as described previously.[12] At the confluence of 80%, the HSMCs culture medium was replaced with a deoxygenated glucose-free DMEM (pH 7.4) and transferred into a hypoxic chamber that perfused with a mixture of 5% $CO_2$ and 95% $N_2$ at 37°C for 12 hours to induce OGD/R insult. Oxygen-glucose deprivation was terminated by replacing the deoxygenated glucose-free DMEM with regular culture medium and incubated in the normal culture conditions (37°C, 5% $CO_2$) for another 18 hours, thus, mimicking reperfusion. Control HSMCs were cultured with standard medium and maintained in normal conditions (37°C, 5% $CO_2$) for equivalent time periods.

### 2.6. Histopathological evaluation

The gastrocnemius muscle specimens were immediately fixed in formalin, embedded in paraffin, and sectioned at 4 μm. After deparafinization and rehydration, the sections were stained with hematoxylin-eosin and examined using a light microscope (Imager Z2, Carl Zeiss, Jena, Germany) by the same experienced pathologist who was blinded to group assignment.

### 2.7. Electron transmission microscope assessment

The cut skeletal muscle tissues were prefixed with 2% glutaraldehyde for 2 hours, postfixed with 1% osmium tetroxide for 1 hour (pH 7.4, 4°C), gradually dehydrated with ethanol, and then embedded in epoxy-resin. Before being evaluated under a H-7650 transmission microscope (Hitachi, Tokyo, Japan), the ultrathin slices (about 70 nm thick) were cut, collected on copper rhodium-coated grids and stained with uranyl acetate and lead citrate.

### 2.8. Detection of caspase activity in muscle tissue

In accordance with the manufacturer's instructions, the muscle tissues were homogenized in the ice-cold lysis buffer and the supernatants were collected to determine the activities of caspase-8 and caspase-9 using colorimetric assay (Abbkine Scientific Co., Ltd, China).

### 2.9. Measurement of plasma interleukin-6 and tumor necrosis factor-α

Blood samples (3 mL) obtained from the abdominal aorta were centrifuged to separate plasma. The plasma levels of IL-6 and TNF-α were determined using an enzyme linked immunosorbent assay in accordance with the manufacturer's protocol (R&D Systems China Co., Ltd., China).

### 2.10. In vivo and in vitro apoptosis assays

Paraffin-embedded skeletal muscle sections were deparaffinized, rehydrated, and permeabilized. After the immersion in equilibration buffer, the sections were incubated with the terminal dUTP nick-end labeling (TUNEL) reaction mixture reagent (Beyotime, Shanghai, China) at 37°C for 1 hour. Subsequently, the slices were stained with 4′, 6-diamidino-2-phenylindole (DAPI) at

room temperature for 5 minutes and proceed to image analysis in five adjacent visual fields in each slice. The percentage of TUNEL-positive cells was calculated relative to the total number of DAPI-positive cells.

Apoptosis analysis of cultured HSMCs was performed using flow cytometry according to the manufacturer's instructions (Beyotime, Shanghai, China). Briefly, HSMCs from each group were washed in PBS three times and resuspended in 400 μL of binding buffer with FITC Annexin V and propidium iodide (PI). Then the cells were placed in the dark at room temperature for 15 minutes, and afterwards, cell apoptosis was analyzed using a BD FACSVerse flow cytometer (BD Biosciences, Franklin Lakes, NJ, USA). The rate of apoptosis was defined as the total percentage of early (Annexin V-positive/PI-negative) and late apoptotic cells (Annexin V-positive/PI-positive).

### 2.11. Western blot

The protein expression of RIPK1, Bok, Bcl-2, and cleaved caspase-3 was detected using Western blot. In brief, identical amounts of protein were obtained from muscle tissues or harvested cells with RIPA lysis buffer containing protease inhibitors, which were then separated by 10% sodium dodecyl sulfate polyacrylamide gel electrophoresis and transferred onto polyvinylidene diflfluoride membranes. After 2 hours of blocking with 5% skimmed milk at 25°C, the membranes were then incubated overnight at 4°C with primary antibodies against RIPK1 (#3493; 1:1000; CST Co.Ltd, USA), Bok (#ab186745; 1:1000; Abcam Co.Ltd, Cambridge, United Kingdom), Bcl-2 (#ab32124; 1:1000; Abcam Co.Ltd, Cambridge, United Kingdom), cleaved caspase-3 (#ab2302; 1:1000; Abcam Co.Ltd, Cambridge, United Kingdom), and GAPDH (#ab8245; 1:1000; Abcam Co.Ltd, Cambridge, United Kingdom). The membranes were washed with Tris-buffered saline buffer with Tween, and then incubated for 2 hours at room temperature with the respective secondary antibodies. Finally, the blots were visualized using ECL reagent and then scanned using the LAS-3000 detection system. The levels of all the target proteins were normalized against GAPDH.

### 2.12. Cell counting kit-8 assay

The cell viability of HSMCs was evaluated using a CCK-8 assay (MCE, Shanghai, China). In brief, HSMCs were cultured in 96-well plates at a density of $1 \times 10^4$ per well. After various treatments following the experimental design, 10 μL CCK-8 solution was added to the medium of each well, and the cells were then incubated again for another 2 hours at 37°C in the dark. Finally, the optical density was detected at a wavelength of 450 nm in a microplate reader (Bio-Rad Laboratories, Inc., USA), and the cell viability was expressed as the percent of control. The experiment was repeated in triplicate.

### 2.13. LDH release assay

Used as a marker of cell injury, LDH release was quantified using commercially available kit (Nanjing Jiancheng Bioengineering Institute, Nanjing, China). The supernatant of HSMCs (120 μL) was collected through centrifugation (400 × g, 5 minutes, room temperature) from each well after corresponding treatment and then transferred to a new plate. Then, LDH detection solution (60 μL) was added to each well. After 30 minutes of incubation at room temperature, the absorbance was measured at a wavelength of 490 nm in a microplate reader (Bio-Rad Laboratories, Inc., USA).

### 2.14. Statistical analysis

SPSS 17.0 software (SPSS Inc., Chicago, IL, USA) was used to analyze the data. Normal distribution of the continuous variables was determined by Kolmogorov-Smirnov test, and the normally distributed data were expressed as mean ± standard deviation. Statistical differences between groups were evaluated using a one-way analysis of variance, followed by the Bonferroni post hoc method. Statistical significance of difference was defined as a $p < 0.05$.

## 3. RESULTS

### 3.1. Nec-1 attenuated IR-induced skeletal muscle damage

Histopathology clearly revealed the existence of regularly arranged myofibers in the muscle section of sham-operated rats, whereas gastrocnemius muscle tissues subjected to IR presented disordered and swollen myofibers of varying diameter, and inflammatory cell infiltration (Fig. 1A). At the ultrastructural level, edema and highly disorganized myofibers were observed, and mitochondrial damage was revealed in muscle tissue subjected to IR as indicated by swelling, the formation of internal vesicles and the disruption or loss of cristae (Fig. 1B). The pretreatment with Nec-1 significantly reduced the microstructural and ultrastructural abnormalities following IR in gastrocnemius muscle tissue.

### 3.2. Nec-1 and Bok knockdown prevented cell injury following OGD/R challenge

It was demonstrated that the OGD/R challenge was attributed to a decrease of cell viability and an increase of LDH release in HSMCs ($p < 0.05$). Nec-1 50 μM significantly attenuated the OGD/R-induced HSMCs injury, as evidenced by the increased cell viability and the decreased LDH release ($p < 0.05$). Similarly, Bok knockdown with siRNA was also found to significantly attenuate OGD/R insult in HSMCs (Fig. 2).

### 3.3. Nec-1 suppressed Bok-mediated apoptosis induced by IR and OGD/R

Numerous TUNEL-positive cells were observed in muscle tissue of rats subjected to IR (Fig. 3A), while the pretreatment with Nec-1 significantly reduced the number of TUNEL-positive cells ($p < 0.05$, Fig. 3B). Moreover, the activities of caspase-8 and caspase-9 in muscle tissue were more significantly enhanced in the IR group than the SM group ($p < 0.05$), which was reduced in the NI group ($p < 0.05$, Fig. 3C). Similar results were presented in vitro, that is, the proportion of the apoptotic (Annexin V-positive/PI-negative and Annexin V-positive/ PI-positive) cells was increased in the OGD/R-treated HSMCs, which was decreased by both Bok knockdown and Nec-1 treatment ($p < 0.05$, Fig. 3D).

### 3.4. RIPK1 acted as an upstream of Bok and caspase-3 activation following IR and OGD/R

Compared with the SM group, the protein levels of RIPK1, Bok and cleaved caspase-3 in the IR and DI groups were increased, and Bcl-2 expression was downregulated in muscle tissue upon reperfusion ($p < 0.05$). The muscular expression of RIPK1, Bok and cleaved caspase-3 was decreased, while Bcl-2 expression was upregulated in rats treated with Nec-1 ($p < 0.05$, Fig. 4A). Similar patterns of RIPK1, Bok and cleaved caspase-3 expression were observed in HSMCs in response to OGD/R, which could be downregulated by Nec-1 incubation ($p < 0.05$, Fig. 4B). Bok knockdown HSMCs presented significantly decreased protein expression of cleaved caspase-3 without compromising RIPK1 expression ($p < 0.05$, Fig. 4B).

### 3.5. Nec-1 decreased the plasma levels of inflammatory cytokines

As expected, Fig. 5 demonstrated that the plasma levels of IL-6 and TNF-α were significantly higher in the IR and DI groups than the SM group ($p < 0.05$), which were dramatically decreased by Nec-1 ($p < 0.05$).

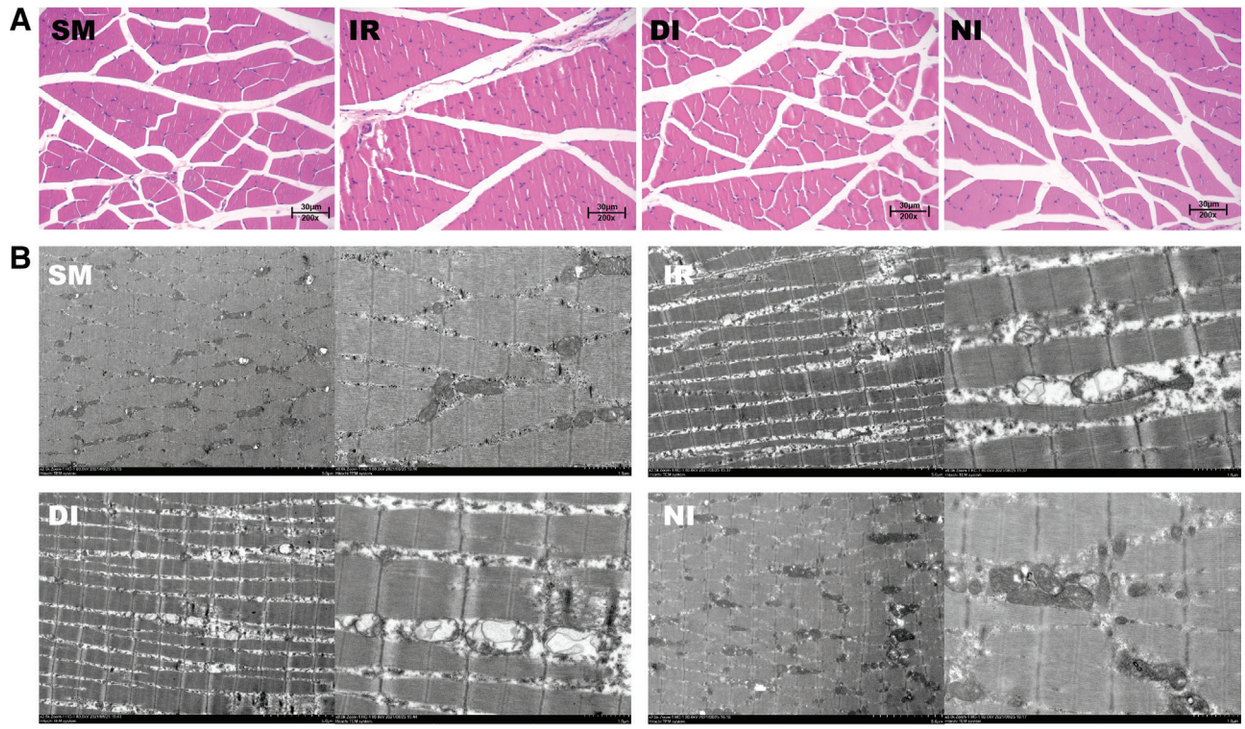


**Fig. 1** Necrostatin-1 attenuated IR-induced skeletal muscle damage. The microstructural (A) and ultrastructural (B) changes of gastrocnemius muscle tissue were evaluated in different groups. DI = ischemia reperfusion + vehicle dimethyl sulfoxide group; IR = ischemia reperfusion group; NI = ischemia reperfusion + Nec-1 group; SM = sham group.

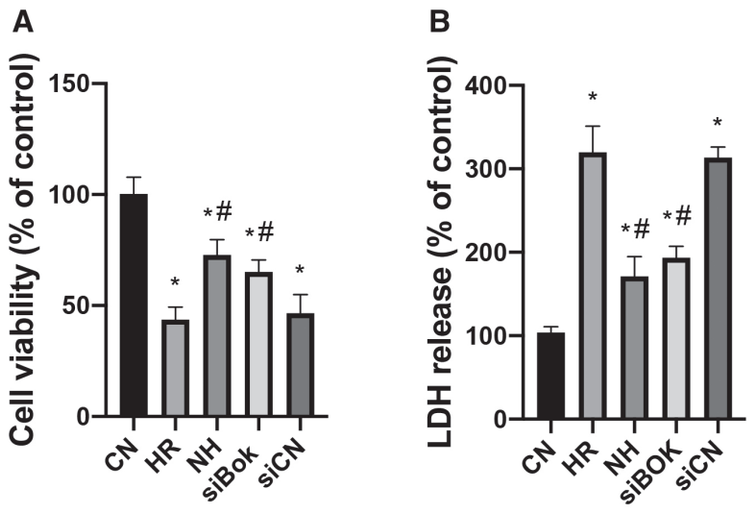


**Fig. 2** Necrostatin-1 and Bok knockdown prevented cell injury following OGD/R challenge. Cell viability (A) and LDH release (B) were measured in HSMCs exposed to OGD/R insult. Data are expressed as means ± standard deviation of three observations, * $p < 0.05$ compared with the CN group; # $p < 0.05$ compared with the HR group. Bok = Bcl-2-related ovarian killer; CN = control group; HR = OGD/R-treated group; HSMCs = human skeletal muscle cells; IR = ischemia reperfusion; LDH = lactate dehydrogenase; NH = Nec-1 + OGD/R group; OGD/R = oxygen-glucose deprivation/ reoxygenation; siBok = Bok siRNA+ OGD/R group; siNC = negative control siRNA + OGD/R group.

## 4. DISCUSSION

It was hereby demonstrated that (1) RIPK1 and Bok were upregulated in skeletal muscle tissue subjected to IR and OGD/R-challenged HSMCs; (2) Nec-1 significantly downregulated the Bok expression, suppressed the caspase activation, attenuated inflammation, and finally attenuated skeletal muscle IR injury; (3) Nec-1 and Bok knockdown protected HSMCs against apoptosis and OGD/R insult. The present results suggested that RIPK1 might act as an upstream regulator of Bok-mediated apoptosis, and that inhibiting RIPK1 with Nec-1 reduced apoptosis in IR-induced skeletal muscle injury at least partly by targeting Bok.

RIPK1 acts as a multifunctional adaptor protein in response to various stimuli, the mechanisms of whose upregulation during reperfusion, however, remain poorly understood. Positive

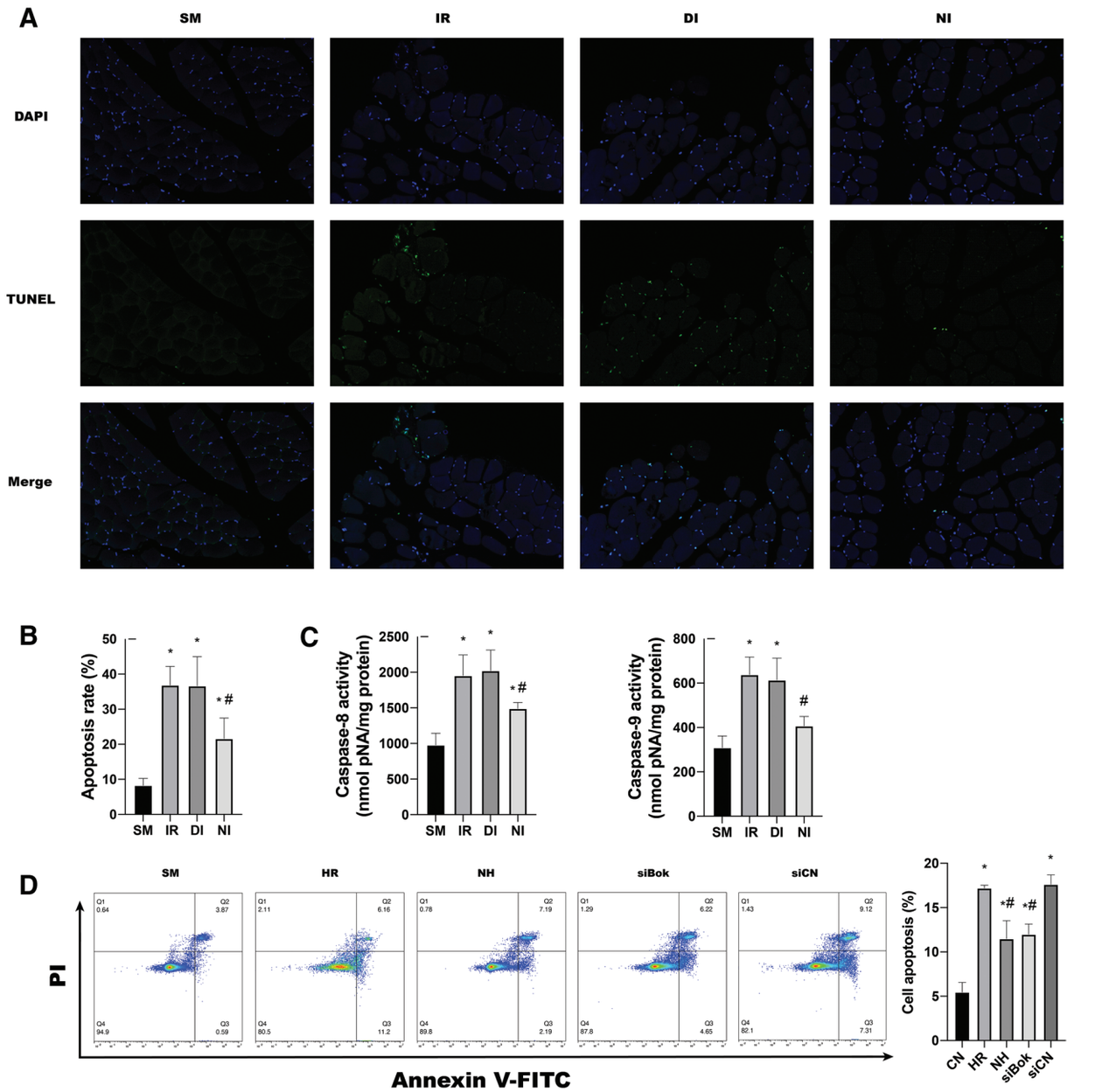


**Fig. 3** Necrostatin-1 suppressed Bok-mediated cell apoptosis induced by IR and OGD/R. TUNEL staining (A), apoptosis rate (B) and activities of caspase-8 and caspase-9 (C) in muscle tissue were measured. Data are expressed as means ± standard deviation of six observations, *$p < 0.05$ compared with the SM group; #$p < 0.05$ compared with the IR group. In vitro, the flow cytometry assay (D) was used to evaluate cell apoptosis in HSMCs, where Annexin V-positive/ PI-negative and Annexin V-positive/ PI-positive cells were apoptotic cells. Data are expressed as means ± standard deviation of three observations, *$p < 0.05$ compared with the CN group; #$p < 0.05$ compared with the HR group. Bok = Bcl-2-related ovarian killer; HSMCs = human skeletal muscle cells; IR = ischemia reperfusion; OGD/R = oxygen-glucose deprivation/ reoxygenation; PI = propidium iodide; TUNEL = terminal dUTP nick-end labeling.

feedback between reactive oxygen species (ROS) and RIPK1 has been demonstrated in the execution of necroptosis,[13,14] and TNF-α treatment and T-cell activation have also been reported to induce RIPK1 expression.[15] In this case, the burst of ROS and TNF-α release may contribute to the upregulated RIPK1 during reperfusion. RIPK1 has multiple domains and distinct molecular functions, where the N-terminal kinase domain involves in mediating the activation of NF-κB, the C terminal domain mediates apoptosis, and its intermediate domain is required for transition between necroptosis and apoptosis.[5,16] In the presence of RIPK1, TNF-α induces the formation of complex I and II, the former of which activates antiapoptotic proteins by activating several signaling pathways, including NF-κB.[17–19] When complex I fails to stimulate NF-κB signaling pathway, TNF-α turns to induce the RIPK1-dependent apoptosis by forming the complex II, which promotes cell death by triggering the caspase cascade,[20,21] thereby mediating the extrinsic apoptotic pathway.[22,23] Importantly, RIPK1 has been suggested to activate caspase-8 through a RIPK1-Fas-associated death domain protein scaffold and promote apoptosis.[24]

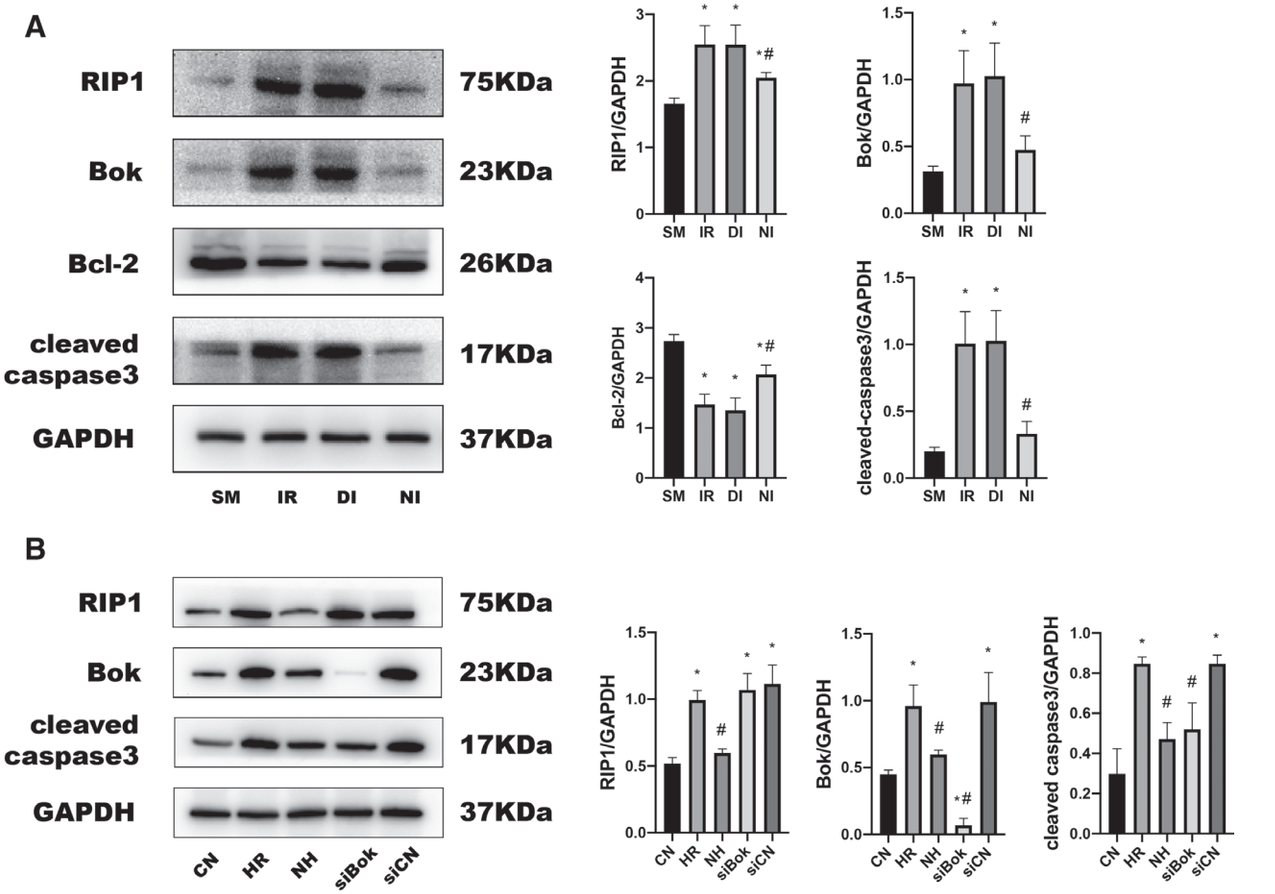


**Fig. 4** RIPK1 regulated Bok and caspase-3 activation following IR and OGD/R. Protein levels of RIPK1, Bok, Bcl-2 and cleaved caspase-3 (A) in muscle tissue were measured. Data are expressed as means ± standard deviation of six observations, *$p < 0.05$ compared with the SM group; #$p < 0.05$ compared with the IR group. In vitro, RIPK1, Bok and cleaved caspase-3 (B) protein expression was also detected in HSMCs. Data are expressed as means ± standard deviation of three observations, *$p < 0.05$ compared with the CN group; #$p < 0.05$ compared with the HR group. RIPK1 = receptor interacting serine/threonine kinase 1; Bok = Bcl-2-related ovarian killer; IR = ischemia reperfusion; OGD/R = oxygen-glucose deprivation/ reoxygenation; Bcl-2 = B-cell lymphoma-2; HSMCs = human skeletal muscle cells.

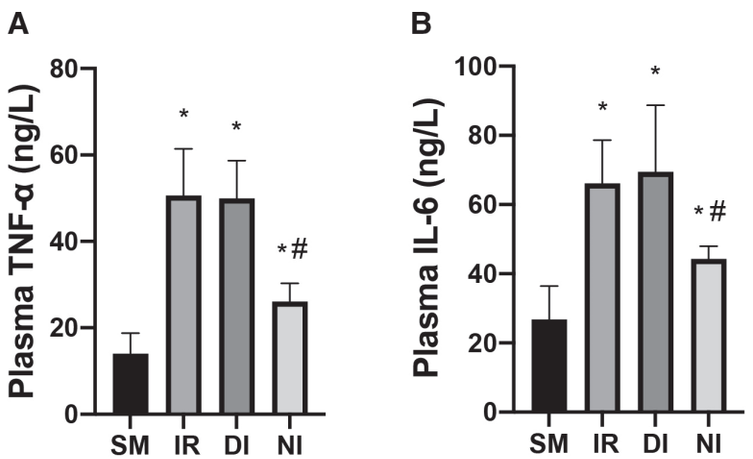


**Fig. 5** Necrostatin-1 decreased the plasma levels of inflammatory cytokines. Plasma levels of TNF-α (A) and IL-6 (B) were determined in rats from different groups. Data are expressed as means ± standard deviation of six observations, *$p < 0.05$ compared with the SM group; #$p < 0.05$ compared with the IR group. IL-6 = interleukin-6; TNF-α = tumor necrosis factor-α.

Considering its crucial role in regulating mitochondrial outer membrane permeabilization,[25] the Bcl-2 family of proteins is well recognized in the intrinsic apoptotic pathway, while Bok is considered a proapoptotic effector due to its roughly 75% sequence similarity to Bax and Bak.[1] However, more than 20 years after its discovery, the exact role of Bok in apoptosis is still not entirely understood or controversially discussed to some extent.[26] As reported, though the exact mechanisms by which IR upregulates Bok expression are undetermined, Bok contributes considerably to IR-induced apoptosis.[27,28] It was hereby assumed that ROS might play important roles, since it would upregulate another Bcl-2 family protein counterpart Bax during IR,[29] and it was shown that overexpression of Bok induced intrinsic apoptosis in a variety of cell types even in the absence of Bax and Bak.[30] By contrast, some studies reported that cell death induced by overexpressed BOK was much reduced in *Bax*$^{-/-}$*Bak*$^{-/-}$ double knockout cells,[3,31] suggesting that BOK induced apoptosis in a Bax and Bak dependent manner. The activation of Bok and its subsequent oligomerization stimulates the pores formation in the mitochondrial outer membrane and increased permeablization, thereby resulting in the release of cytochrome c and the activation of proapoptotic molecules such as caspase-3.[3,32,33]

As demonstrated previously, RIPK1 deficiency inhibited the poly (ADP-ribose) polymerase-1 (PARP-1)-induced c-Jun N-terminal kinase (JNK) activation and contributed to increased resistance against mitochondrial dysfunction and apoptosis, indicating the role of RIPK1 as an upstream regulator of PARP-1-activated JNK.[34] This was also supported by Zhang et al,[35] who demonstrated that RIPK1-mediated apoptosis signal-regulating kinase 1-interacting protein 1 (AIP1) phosphorylation at the 14-3-3-binding site Ser-604 was required for the formation of the apoptotic complex and the activation of apoptotic JNK/p38 signaling in response to TNF-α. Furthermore, RIPK1 induced the phosphorylation of extracellular signal-regulated kinase (ERK) following eleostearic acid exposure, thus leading to ROS overproduction and mitochondrial dysfunction.[19] Taken together, these results confirmed the crucial role of mitogen-activated protein kinases activation in RIPK1-dependent apoptosis by targeting Bcl-2 family proteins.

Nec-1, a small tryptophan-based molecule and a selective allosteric inhibitor of RIPK1, is capable of inhibiting necroptosis triggered by the dimerization of the kinase domain.[36] It was hereby indicated that Nec-1 treatment downregulated the protein expression of total RIPK1, which was consistent with previous studies.[37,38] Different from its definite anti-necroptotic action, the effects of Nec-1 on apoptosis are debatable. Several studies have demonstrated that Nec-1 inhibited apoptosis.[10,39] Nec-1 drastically lowered the expression of apoptosis-related proteins while increasing the expression of the antiapoptotic protein Bcl-2, and decreased the number of apoptotic cells in the hippocampus CA1 region of mice with status epilepticus.[39] Additionally, similar results were presented when rats were administered with Nec-1 to prevent spinal cord damage.[10] Indeed, the current study demonstrated that the pretreatment with Nec-1 reduced muscular Bok expression and restrained apoptosis following IR. Furthermore, Nec-1 treatment and Bok knockdown blunted apoptosis and OGD/R-induced skeletal muscle cell injury. Thus, it is believed that Nec-1 therapy attenuated IR-induced skeletal muscle damage by regulating Bok-mediated apoptosis. However, opposite results have been reported in some other studies. For instance, Nec-1 was capable of inducing apoptotic neutrophil death, which reduced the chronic inflammation.[40] Interestingly, Nec-1 significantly increased the liver damage and decreased the survival time in septic rats by permitting the apoptotic pathway, demonstrating that Nec-1 might lead to unfavorable consequences beside its therapeutic purposes.[41] It was also assumed that various pathophysiological situations would give rise to tissue damage with distinct properties and varied cell death patterns, which might reasonably explain the paradoxical effects of Nec-1 on apoptosis.

Several limitations of the present study should be noticed. First, the dosage of the chosen Nec-1 referred to published study,[42] but the single dosage of Nec-1 possibility led to inadequate inhibition of RIPK1 by Nec-1. Second, the precise mechanisms involved in regulating Bok activation by RIPK1 were not studied in the present study, and the phosphorylated form of RIPK1 was not measured, either. Third, Nec-1 was administered before ischemia initiation in the present study, which might be differed from clinical scenarios, and the effects of Nec-1 administration after ischemia should be studied as well. Finally, this study failed to exclude the RIPK1-independent mechanisms that might contribute to the protective effects of Nec-1, since targets of Nec-1 activity other than RIPK1 have also been suggested. For instance, Nec-1 inhibited nitric oxide donor-induced β-cells cell death via the activation of protein kinase B (Akt) in a RIPK1-independent manner,[43] while Akt is a well-known kinase involved in the regulation of apoptosis in skeletal muscle IR.[44,45]

It is concluded that inhibiting RIPK1 with Nec-1 did prevent skeletal muscle from IR injury by targeting Bok-mediated apoptosis.

## ACKNOWLEDGMENTS

The study was funded by Wenzhou Municipal Science and Technology Bureau [grant numbers Y20180123, Y2020225]. The funding agency had no role in study design, collection/analyses of data, decision to publish, or article preparation.

## REFERENCES

1. Hsu SY, Kaipia A, McGee E, Lomeli M, Hsueh AJ. Bok is a pro-apoptotic Bcl-2 protein with restricted expression in reproductive tissues and heterodimerizes with selective anti-apoptotic Bcl-2 family members. *Proc Natl Acad Sci U S A* 1997;**94**:12401–6.
2. Rodriguez JM, Glozak MA, Ma Y, Cress WD. Bok, Bcl-2-related Ovarian Killer, Is Cell Cycle-regulated and Sensitizes to Stress-induced Apoptosis. *J Biol Chem* 2006;**281**:22729–35.
3. Echeverry N, Bachmann D, Ke F, Strasser A, Simon HU, Kaufmann T. Intracellular localization of the BCL-2 family member BOK and functional implications. *Cell Death Differ* 2013;**20**:785–99.
4. Galluzzi L, Kepp O, Chan FK, Kroemer G. Necroptosis: Mechanisms and Relevance to Disease. *Annu Rev Pathol* 2017;**12**:103–30.
5. Ofengeim D, Yuan J. Regulation of RIP1 kinase signalling at the crossroads of inflammation and cell death. *Nat Rev Mol Cell Biol* 2013;**14**:727–36.
6. Chen J, Kos R, Garssen J, Redegeld F. Molecular insights into the mechanism of necroptosis: the necrosome as a potential therapeutic target. *Cells* 2019;**8**:E1486.
7. Liao S, Apaijai N, Chattipakorn N, Chattipakorn SC. The possible roles of necroptosis during cerebral ischemia and ischemia / reperfusion injury. *Arch Biochem Biophys* 2020;**695**:108629.
8. Zhang X, Wu J, Liu Q, Li X, Li S, Chen J, et al. mtDNA-STING pathway promotes necroptosis-dependent enterocyte injury in intestinal ischemia reperfusion. *Cell Death Dis* 2020;**11**:1050.
9. Zhang T, Zhang Y, Cui M, Jin L, Wang Y, Lv F, et al. CaMKII is a RIP3 substrate mediating ischemia- and oxidative stress-induced myocardial necroptosis. *Nat Med* 2016;**22**:175–82.
10. Wang Y, Wang H, Tao Y, Zhang S, Wang J, Feng X. Necroptosis inhibitor necrostatin-1 promotes cell protection and physiological function in traumatic spinal cord injury. *Neuroscience* 2014;**266**:91–101.
11. Zhang F, Ren L, Zhou S, Duan P, Xue J, Chen H, et al. Role of B-Cell Lymphoma 2 Ovarian Killer (BOK) in acute toxicity of human lung epithelial cells caused by cadmium chloride. *Med Sci Monit* 2019;**25**:5356–68.
12. Ettinger K, Lecht S, Arien-Zakay H, Cohen G, Aga-Mizrachi S, Yanay N, et al. Nerve growth factor stimulation of ERK1/2 phosphorylation requires both p75NTR and α9β1 integrin and confers myoprotection

towards ischemia in C2C12 skeletal muscle cell model. *Cell Signal* 2012;**24**:2378–88.
13. Zhang Y, Su SS, Zhao S, Yang Z, Zhong CQ, Chen X, et al. RIP1 autophosphorylation is promoted by mitochondrial ROS and is essential for RIP3 recruitment into necrosome. *Nat Commun* 2017;**8**:14329.
14. Lu B, Gong X, Wang ZQ, Ding Y, Wang C, Luo TF, et al. Shikonin induces glioma cell necroptosis in vitro by ROS overproduction and promoting RIP1/RIP3 necrosome formation. *Acta Pharmacol Sin* 2017;**38**:1543–53.
15. Stanger BZ, Leder P, Lee TH, Kim E, Seed B. RIP: a novel protein containing a death domain that interacts with Fas/APO-1 (CD95) in yeast and causes cell death. *Cell* 1995;**81**:513–23.
16. Festjens N, Vanden Berghe T, Cornelis S, Vandenabeele P. RIP1, a kinase on the crossroads of a cell's decision to live or die. *Cell Death Differ* 2007;**14**:400–10.
17. Varfolomeev E, Vucic D. (Un)expected roles of c-IAPs in apoptotic and NFkappaB signaling pathways. *Cell Cycle* 2008;**7**:1511–21.
18. Darding M, Meier P. IAPs: guardians of RIPK1. *Cell Death Differ* 2012;**19**:58–66.
19. Obitsu S, Sakata K, Teshima R, Kondo K. Eleostearic acid induces RIP1-mediated atypical apoptosis in a kinase-independent manner via ERK phosphorylation, ROS generation and mitochondrial dysfunction. *Cell Death Dis* 2013;**4**:e674.
20. Micheau O, Tschopp J. Induction of TNF receptor I-mediated apoptosis via two sequential signaling complexes. *Cell* 2003;**114**:181–90.
21. Ranjan K, Pathak C. FADD regulates NF-κB activation and promotes ubiquitination of cFLIPL to induce apoptosis. *Sci Rep* 2016;**6**:22787.
22. Wang L, Du F, Wang X. TNF-alpha induces two distinct caspase-8 activation pathways. *Cell* 2008;**133**:693–703.
23. Tenev T, Bianchi K, Darding M, Broemer M, Langlais C, Wallberg F, et al. The Ripoptosome, a signaling platform that assembles in response to genotoxic stress and loss of IAPs. *Mol Cell* 2011;**43**:432–48.
24. Abhari BA, Cristofanon S, Kappler R, von Schweinitz D, Humphreys R, Fulda S. RIP1 is required for IAP inhibitor-mediated sensitization for TRAIL-induced apoptosis via a RIP1/FADD/caspase-8 cell death complex. *Oncogene* 2013;**32**:3263–73.
25. Lossi L. The concept of intrinsic versus extrinsic apoptosis. *Biochem J* 2022;**479**:357–84.
26. Naim S, Kaufmann T. The Multifaceted Roles of the BCL-2 family member BOK. *Front Cell Dev Biol* 2020;**8**:574338.
27. Di G, Yang X, Cheng F, Liu H, Xu M. CEBPA-AS1 knockdown alleviates oxygen-glucose deprivation/reperfusion-induced neuron cell damage by the MicroRNA 24-3p/BOK Axis. *Mol Cell Biol* 2021;**41**:e0006521.
28. Nakajima Y, Shimazawa M, Mishima S, Hara H. Neuroprotective effects of Brazilian green propolis and its main constituents against oxygen-glucose deprivation stress, with a gene-expression analysis. *Phytother Res* 2009;**23**:1431–8.
29. Sun L, Fan H, Yang L, Shi L, Liu Y. Tyrosol prevents ischemia/reperfusion-induced cardiac injury in H9c2 cells: involvement of ROS, Hsp70, JNK and ERK, and apoptosis. *Molecules* 2015;**20**:3758–75.
30. Einsele-Scholz S, Malmsheimer S, Bertram K, Stehle D, Johänning J, Manz M, et al. Bok is a genuine multi-BH-domain protein that triggers apoptosis in the absence of Bax and Bak. *J Cell Sci* 2016;**129**:2213–23.
31. Carpio MA, Michaud M, Zhou W, Fisher JK, Walensky LD, Katz SG. BCL-2 family member BOK promotes apoptosis in response to endoplasmic reticulum stress. *Proc Natl Acad Sci U S A* 2015;**112**:7201–6.
32. Kuwana T, Mackey MR, Perkins G, Ellisman MH, Latterich M, Schneiter R, et al. Bid, Bax, and lipids cooperate to form supramolecular openings in the outer mitochondrial membrane. *Cell* 2002;**111**:331–42.
33. Scorrano L, Ashiya M, Buttle K, Weiler S, Oakes SA, Mannella CA, et al. A distinct pathway remodels mitochondrial cristae and mobilizes cytochrome c during apoptosis. *Dev Cell* 2002;**2**:55–67.
34. Xu Y, Huang S, Liu ZG, Han J. Poly(ADP-ribose) polymerase-1 signaling to mitochondria in necrotic cell death requires RIP1/TRAF2-mediated JNK1 activation. *J Biol Chem* 2006;**281**:8788–95.
35. Zhang H, Zhang R, Zhang H, Lin Y, Li J, Pober JS, et al. RIP1-mediated AIP1 phosphorylation at a 14-3-3-binding site is critical for tumor necrosis factor-induced ASK1-JNK/p38 activation. *J Biol Chem* 2007;**282**:14788–96.
36. Degterev A, Huang Z, Boyce M, Li Y, Jagtap P, Mizushima N, et al. Chemical inhibitor of nonapoptotic cell death with therapeutic potential for ischemic brain injury. *Nat Chem Biol* 2005;**1**:112–9.
37. Wen S, Ling Y, Yang W, Shen J, Li C, Deng W, et al. Necroptosis is a key mediator of enterocytes loss in intestinal ischaemia/reperfusion injury. *J Cell Mol Med* 2017;**21**:432–43.
38. Ashour H, Hashem HA, Khowailed AA, Rashed LA, Hassan RM, Soliman AS. Necrostatin-1 mitigates renal ischaemia-reperfusion injury - time dependent - via aborting the interacting protein kinase (RIPK-1)-induced inflammatory immune response. *Clin Exp Pharmacol Physiol* 2022;**49**:501–14.
39. Lin DQ, Cai XY, Wang CH, Yang B, Liang RS. Optimal concentration of necrostatin-1 for protecting against hippocampal neuronal damage in mice with status epilepticus. *Neural Regen Res* 2020;**15**:936–43.
40. Jie H, He Y, Huang X, Zhou Q, Han Y, Li X, et al. Necrostatin-1 enhances the resolution of inflammation by specifically inducing neutrophil apoptosis. *Oncotarget* 2016;**7**:19367–81.
41. Zhang Q, Wei S, Lu J, Fu W, Chen H, Huang Q, et al. Necrostatin-1 accelerates time to death in a rat model of cecal ligation and puncture and massively increases hepatocyte caspase-3 cleavage. *Am J Physiol Gastrointest Liver Physiol* 2019;**316**:G551–61.
42. Reddy AS, Abraham A, McClain SA, Clark RA, Ralen P, Sandoval S, et al. The role of necroptosis in burn injury progression in a rat comb burn model. *Acad Emerg Med* 2015;**22**:1181–6.
43. Tamura Y, Chiba Y, Tanioka T, Shimizu N, Shinozaki S, Yamada M, et al. NO donor induces Nec-1-inhibitable, but RIP1-independent, necrotic cell death in pancreatic β-cells. *FEBS Lett* 2011;**585**:3058–64.
44. Zhong J, Sun Y, Han Y, Chen X, Li H, Ma Y, et al. Hydrogen sulfide-loaded microbubbles combined with ultrasound mediate thrombolysis and simultaneously mitigate ischemia-reperfusion injury in a rat hindlimb model. *J Thromb Haemost* 2021;**19**:738–52.
45. Shen GH, Song Y, Yao Y, Sun QF, Jing B, Wu J, et al. Downregulation of DLGAP1-antisense rna 1 alleviates vascular endothelial cell injury via activation of the phosphoinositide 3-kinase/akt pathway results from an acute limb ischemia rat model. *Eur J Vasc Endovasc Surg* 2020;**59**:98–107.